JOURNAL OF MATERIALS SCIENCE **36** (2001) 3061 – 3066

Preparation of porous hydroxyapatite

JINTAO TIAN, JIEMO TIAN
Beijing Fine Ceramic Laboratory, INET, Tsinghua University, P. O. Box 1021 Beijing 102201, People's Republic of China
E-mail: jttian@263.net

The aim of the paper was to obtain a porous hydroxyapatite (HA) biomaterials relating to the manufacture of artificial implants. The technique of impregnating a body of porous polyurethane foam with slurry containing HA powder, water and additives was applied and proved to be more successful. The process of preparations was discussed and the porous HA with desired properties was obtained at last.

1. Introduction

Over the past decades of years hydroxyapatite [$Ca_{10}(PO_4)_6(OH)_2$, HA] and related calcium phosphate ceramic materials have been widely used as implant materials due to their close similarity in composition and highly biocompatibility with nature bone [1–3]. Such bioactive implant materials can be applied both in the compact and porous forms as well as granules. In the case of porosint a number of *in vivo* studies have demonstrated the occurrence of bone formation in the pores of the calcium phosphate ceramics such as hydroxyapatite/β-tricalcium phosphate (HA/β-TCP)[4, 5]. However, most of the investigations on the implantation of the porous calcium phosphate ceramics showed that the degree of infiltration of living tissue into the pores and formation of new bone depended greatly on the pore characteristics such as porosity, pore size, pore size distribution and pore shape [6, 7]. Hulbert *et al*. [8] claimed that a minimum pore size of 100 micrometers is necessary for the porous implant materials to function well and pore size greater than 200 micrometers is an essential requirement for osteoconduction.

A lot of methods have been developed to fabricate the porous HA(or HA/β–TCP) ceramics with diversified pore characteristics. There include incorporation of volatile or combustible burn-outs that are lost during firing, solid-state sintering, sol-gel process and reticulated open-celled ceramics produced via the replication of a porous substrate, which is the most common approach for producing open-cell porous ceramics [9]. The porous ceramics obtained from reticulated polymer substrates have a variety of unique properties such as controllable pore size, controllable tortuosity and complex ceramic shapes for different applications.

This paper investigated the technology of obtaining open-cell macroporous calcium phosphate ceramics (average pore size larger than 200 micrometers) based on the replication of a porous substrate. The preparing process was discussed and the open-cell macroporous calcium phosphate bioceramics with desirable properties were obtained at last.

2. Experiment

2.1. Raw materials

The precursor powder of HA was synthesized by wet chemical method in accordance with:

$$10Ca(NO_3)_2 + 6(NH_4)_3PO_4 + 2NH_3 \cdot H_2O = Ca_{10}(PO_4)_6(OH)_2 + 20NH_4NO_3$$

The preparing process of HA powder included the following steps: (i) Preparation of $Ca(NO_3)_2$ solution and $(NH_4)_3PO_4$ solution with appropriate concentrations; (ii) The $Ca(NO_3)_2$ solution was added in drops into the $(NH_4)_3PO_4$ solution in a stoichiometric proportion and stirred at the temperature of 90 °C; (iii) Meanwhile, $NH_3 \cdot H_2O$ Solution was added to keep pH value no less than 9; (iv) The gelatinous sediments were filtered and washed several times until the pH value equal to 7 approximately; (v)The sediments were dried at 110 °C for 3 hr and calcified at 700 °C for 3 hr; (vi) The calcified sediments were dispersed in ethanol solvent and ground for 24 hr: (vii) The ground powder was dried in air.

The obtained powder was analyzed by SA-CP3 particle size analyzer and the result was given in Fig. 1. Fig. 1 shows that the powder particles have an average size of about one micrometer. The scanning electron microscope (SEM) micrograph of the precursor powder was shown in Fig. 2. The XRD analysis of the powder shows a crystallographic structure closely resembling that of hydroxyapatite (JCPDS #9-432), as illustrated in Fig. 3. A sequential X-ray fluorescence spectrometer (Made in Shimadzu, Japan) was used to obtain the powder's calcium to phosphate ratio (Ca/P ratio). Table I shows a value of 1.677, the same thing to hydroxyapatite. Fig. 3 and Table I demonstrate that the precursor powder synthesized above was pure hydroxyapatite.

In order to improve the sintering performance and mechanical properties of porous HA some nano-scale ceramics such as silicon carbide and magnesia were used in the experiments. Other organic agents used as additives were analytically pure.

TABLE I Ca/P ratio of HA powder and porous HA

	Ca	P	Ca/P
HA powder	34.24	20.42	1.677
Porous HA	31.07	18.52	1.678

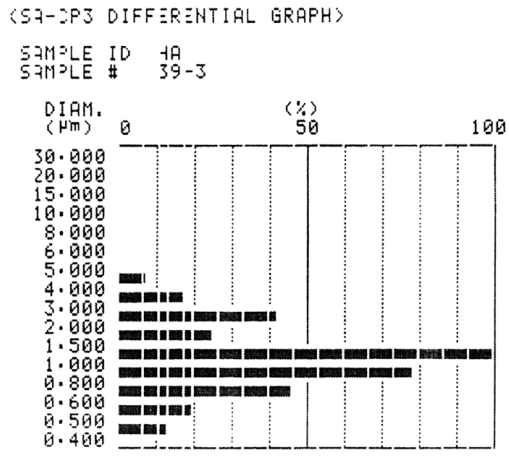

Figure 1 Particle size distribution of HA powder.

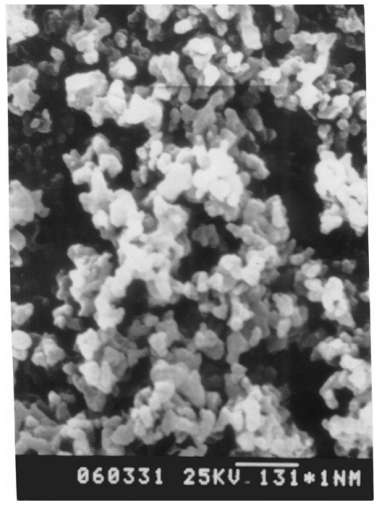

Figure 2 SEM micrograph of HA powder.

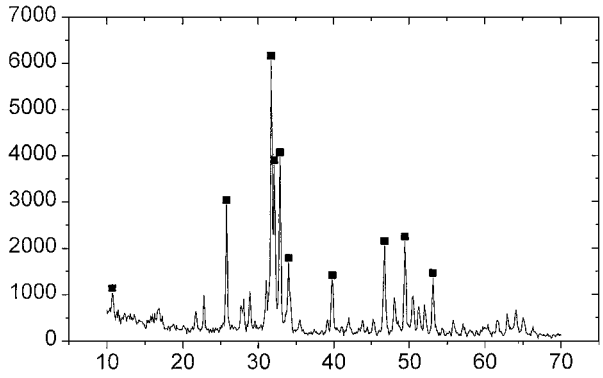

Figure 3 XRD pattern of HA powder.

2.2. Experimental procedure

The experimental procedure is showed schematically in Fig. 4. In order to obtain an open-cell macroporous HA, a suitable reticulated substrate should be selected at first. Then, a ceramic slurry was prepared and coated onto the substrate. After that, the porous samples were dried and sintered carefully. The sintered samples were machined, washed and sterilized. The details will be described in the following.

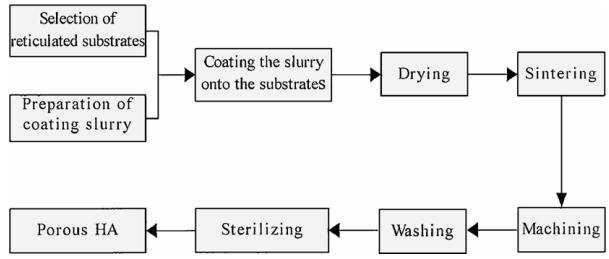

Figure 4 Preparing procedure of porous HA.

2.2.1. Selection of reticulated substrate

In order to obtain an open-cell macroporous HA based on the replication of a porous substrate, a body of organic foam should be adopted as substrate, which was impregnated with ceramic slurry and burned out during the sintering. The organic foam should have an open-cell porous structure. Moreover, the foam should also be:

①able to recover their original shape successfully after impregnation;
②easily and thoroughly eliminated at a temperature of less than 1200 °C which is the sintering temperature of HA;
③able to vary its pore size upon requirements of the products.

There are several types of organic foam which could match the requirements described above very well, such as polyurethane and polyvinyl chloride. The polyurethane used in our experiments has enough recovering ability and could be thoroughly burned out during sintering. Fig. 5 shows the porous structure of the polyurethane substrate. In the case shown in Fig. 5 the polyurethane substrate is composed of a large number of interconnecting pores. The pores are of characteristics of open cell, well-distributed pore size and homogeneous pore distribution that determine the final structures of porous ceramics.

The polyurethane substrate was formed into desired shape depending on the particular applications.

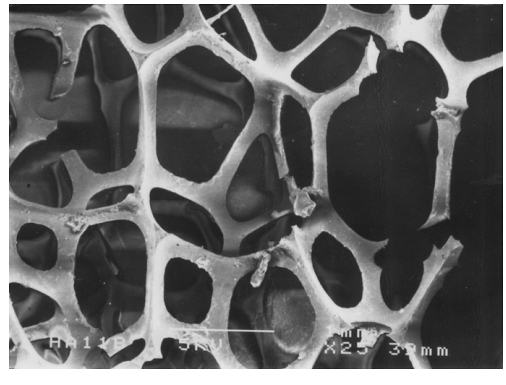

Figure 5 Porous structure of polyurethane substrate.

TABLE II Composition of slurry (wt%)

Component	Content (wt%)
Hydroxyapatite	40%
Silicon carbide	2.5%
Magnesia	2.5%
Binder	1 ~ 5%
Antifoaming agent	1 ~ 3
Distilled water	40 ~ 50

2.2.2. Preparation of coating slurry

The slurry used in the experiments was made up to the recipe given in the Table II.

In Table II, the additions of magnesia and silicon carbide conduce to the improvements of the sintering performance and mechanical properties of porous HA. The binder agent can become the slurry adherent to the substrate while the antifoaming agent can reduce the tendency of formation of "bridge" and "cell walls" [10]. All the ingredients were put in a jar with alumina grinding media and milled for an hour. The resulting slurry was suitable for coating.

2.2.3. Coating the slurry onto the substrate

In this step, the organic foam was dipped into the ceramic slurry and withdrawn. Surplus slurry was removed by centrifuging and the foam was dried in air. The dried foam was then dipped into the slurry again, centrifuged and dried. Similar operations could be repeated till a desirable ceramic coating was obtained at last.

The difficulty encountered during the impregnation was the tendency of the ceramic slurry to drain almost completely from parts of the foam structure due to interfacial phenomena between the slurry and the substrate. As a result, the deposit of ceramic slurry was thinner than was desirable and its thickness was also extremely variable. Additionally in reticulated foam the slurry tended to accumulate at the joint points between rods of polymer rather than along the length of the rods themselves.

In order to solve these problems mentioned above and form a satisfactory coating of ceramic particles on the foam, a kind of flocculating agent was employed during the coating process. The flocculating agent was prepared in accordance with:

$$2AlCl_3 + 5NH_3 \cdot H_2O \rightarrow Al_2(OH)_5Cl + 5NH_4Cl$$

Fig. 6 shows the preparing procedure. The prepared flocculating agent has a pH value of 5 ~ 6.

Before impregnation the substrate was pretreated with the flocculating agent. When the so-treated substrate was dipped into the ceramic slurry having a pH value of 9 ~ 10, a local gelatinous precipitate of $Al(OH)_3$ would be generated on the interface between the slurry and the substrate. The formed precipitate of $Al(OH)_3$ did not then readily redisperse into the slurry and occluded suspended ceramics particles to drain from substrate. The treated/coated circle was repeated as many time as necessary and the desirable

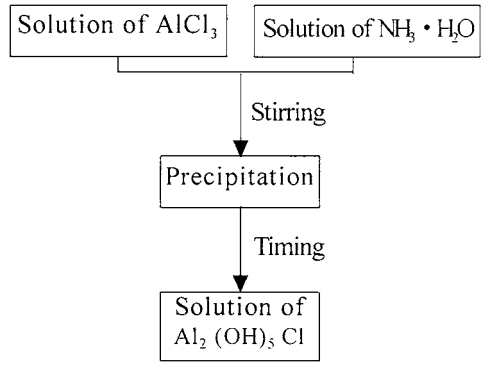

Figure 6 Preparing procedure of the flocculating agent

coating with a continuous and uniform thickness would be formed at last.

2.2.4. Drying and sintering

After coated the samples were dried in air. The time for air-drying was always no less than 24 hr.

The porous samples were sintering at the temperature of 1200 °C. During sintering, the organic substrate began to decompose at the temperature of 200 °C–300 °C and lost its supporting function. The samples without substrate supporting have a weak strength and easily to be destroyed before sintered. The porous samples obtained in the experiments have a large sintering shrinkage of about 30%. If the porous samples couldn't shrink freely during sintering, large cracks always generated during sintering.

In order to solve the problem of shrinking freely during sintering and obtain porous HA without cracks, a special sintering process was carefully planned, schematically showed in Fig. 7. In the case shown in Fig. 7, a compact sheet of HA having a sintering shrinkage of about 15% was placed in the oven and could shrink freely during sintering. On the compact sheet, a porous cushion was placed. The porous sample of HA was finally placed on the cushion. The cushion has a shrinkage of about 30%, similar with that of the porous sample. During sintering, the compact sheet fully shrank and contributed to the shrinkage of the bottom of the cushion, where small cracks would be formed because of partially shrinkage. However, the top surface of the cushion hasn't any resistance and shrink easily. As a result, the porous sample of HA placed on the cushion could shrink freely. The preparations and

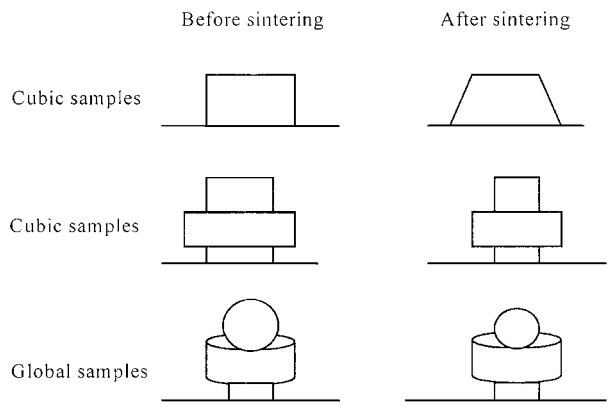

Figure 7 Placements of porous HA in the oven during sintering.

TABLE III A special sintering process for porous HA

Sintering	Method of preparation	Shrinkage content in the level	Character of shrinking
Porous samples on the top	Impregnating a foam with ceramic slurry	∼30%	Fully
Porous cushion in the middle	Impregnating a foam with ceramic slurry	19 ∼ 30%	Fully on the top surface Partially at the bottom surface
Compact sheet at the bottom	Pressed in a model	∼15%	Fully

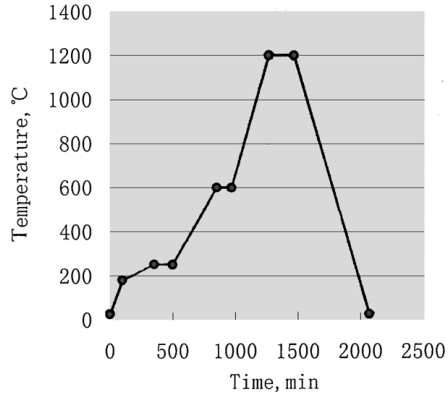

Figure 8 The heating speed of porous HA during sintering.

relevant shrinkage of the sheet and the cushion were given in Table III.

Another attention during sintering was the heating speed. The temperature should be increased slowly so as to make the substrate decompose gradually and avoid cracks formation, especially in the low temperature stage. The heating curve adopted in the experiments was showed in Fig. 8.

2.2.5. Machining, washing and sterilizing

The porous HA could be little machined because the shapes of the samples have already been obtained via the shapes of the foam. After machined, the samples were washed by ultrasonic and sterilized by Co60 radial (25 kGry).

3. Results and discussion

3.1. Phase composition and macrostructure of porous HA

Fig. 9 shows the XRD analysis result. The porous samples sintered in air almost lost their carboxyl and converted into β-tricalcium phosphate (β-TCP). However, the porous samples sintered in vapor have a HA content of about 80%. In the case of sintering in vapor, the conversion of HA into β-TCP is obstructed strongly. The porous samples have a Ca/P ratio of 1.678, shown in Table I.

The macrostructure of the porous HA was controlled by the porous structure of the polymer substrate. Corresponding to the structure of the polymer substrate selected in the experiments (Fig. 5), Figs 10 and 11 illustrate the resulting macrostructure of the porous HA.

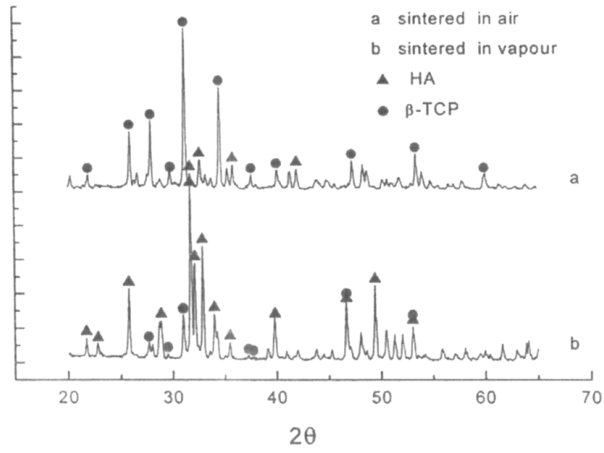

Figure 9 XRD pattern of porous HA.

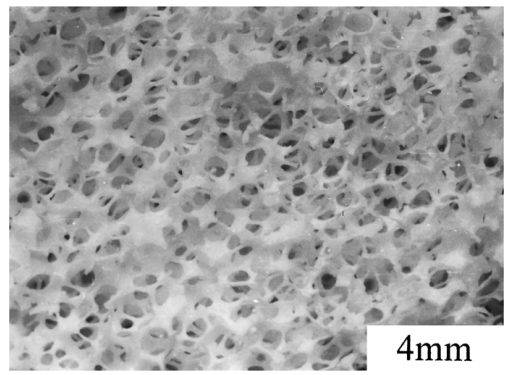

Figure 10 Porous structure of HA from foam of YG-40(5x).

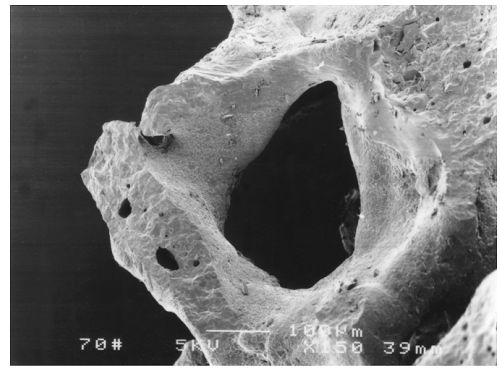

Figure 11 A single pore of HA from foam of YG-70.

They had circular open-cell pores and the pore structure resembling that of the original polymer substrate.

3.2. Influence of content of the slurry

Based on the coating process mentioned above, Tables IV and V show some experimental data for the content of slurry and pore size of the foam.

In the case shown in Table IV, a body of porous polymer foam of pore size YG-70 was selected as impregnating substrate. Three different contents of the slurry, 1, 0.75, and 0.65, were adopted. The values of the porosity from 58% to 80% showed an increasing tendency with the decrease of the content of the slip, while the content of 0.75 and porosity of 75% were preferable.

TABLE IV Experimental data for different slurry content

Content of slurry per one cm^3 of foam (g/cm^3)	Weight of foam after impregnating (g)	Weight of porous HA after sintering (g)	Volume of HA after sintering (cm^3)	Porosity
1	20.9	9	8.9	58%
0.75	15.9	6.7	9.5	75%
0.65	13.9	5.9	9.9	80%

TABLE V Experimental data for different pore size foam

Sorts of foam	Pore size of foam (mm)	Content of slurry per one cm^3 of foam (g/cm^3)	Pore size of HA produces (mm)	Porosity
YG-40	~0.7	0.75	~0.4	80.1%
YG-70	~0.4	0.75	~0.25	78%
YG-100	~0.25	0.75	~0.15	75%

3.3. Influence of pore size of substrate

Three different polymer substrates with different pore size of YG-40, YG-70, and YG-100 were selected in Table V. Figs 12 and 13 show the microstructures of the obtained porous HA. The differences between Figs 12 and 13 were not only the pore size which was resulted from the pore size of substrate but also the former possessed a lot of cracks. However. adopting the porous substrate of small pore size (Fig. 13) could easily reduce these cracks. This was due to the fact that the cracks were caused by the pyrolysis of the polymer substrate while the polymer substrate having small pore size possessed thinner struts and were easily pyrolysied than that of large pore size. Moreover, drying and sintering carefully were conducive to the cracks reducing.

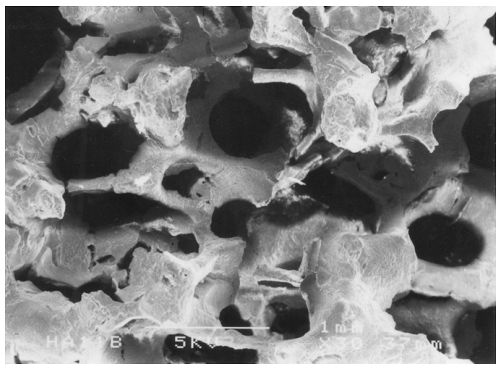

Figure 12 SEM morphology of porous HA from foam of YG-40.

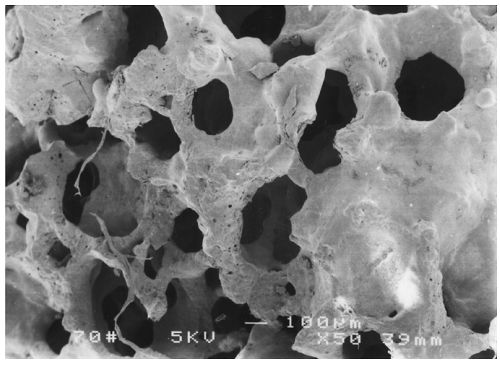

Figure 13 SEM morphology of porous HA from foam of YG-70.

3.4. Mechanical properties

Porous samples with dimensions of $20 \times 20 \times 20\ mm^3$ were tested in compression on an servo tester (Model MTS810. USA) at a crosshead feed rate of l mm/min.

For porous materials, the properties related directly to the porosity and their relationship could be described by D. M. Liu [11] as Equation 1:

$$(\text{Property}) = (\text{property})_0 * \exp^{-b*p} \tag{1}$$

Porous HA with different porosity obtained in the experiments were tested in compression and the results were showed in Fig. 14. In the case shown in Fig. 14, the compressive strength decreased markedly with the porosity increasing. The fitting curve has an exponential tendency and is showed in Equation 2:

$$\begin{aligned} Y &= 14.6 * \exp^{(0.36-x)/0.15} \\ &= 161 * \exp^{-6.7*x} \end{aligned} \tag{2}$$

With Equation 2 the porous HA with desirable compressive strength and suitable porosity could be designed and prepared according to the clinical requirements.

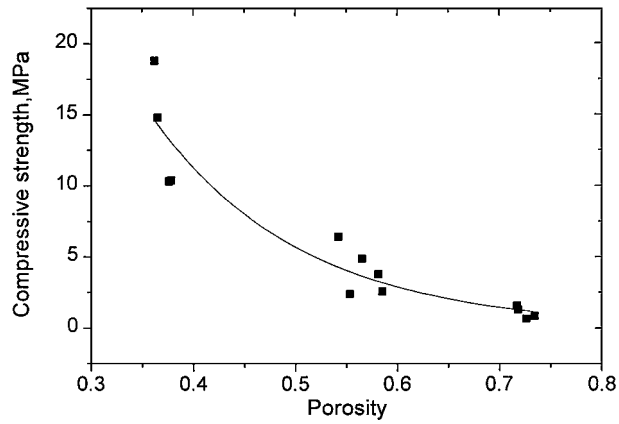

Figure 14 Compressive strength of porous HA.

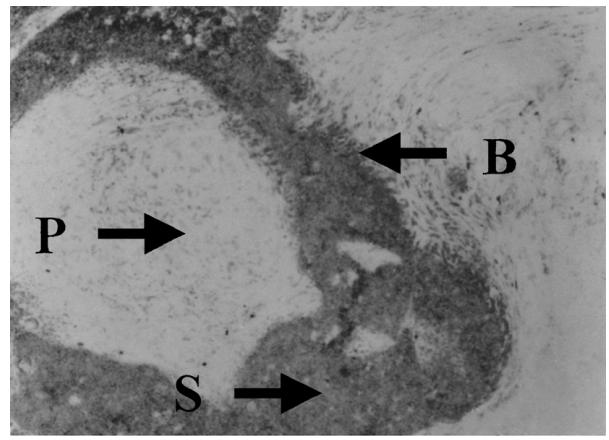

Figure 15 Specimen from porous HA, thirty days after implantation (P: pore in the porous HA; S: skeleton of the porous HA; B: bone tissue).

3.5. Animal experiments

The porous HA with marrow cell fostered after sterilization was implanted into dorsal muscular tissues of rat for animal experiments. The implanted sites of the rats did not show any infection and inflammation. Fig. 15 shows the experimental results. From Fig. 15 we know that the bone tissue, bone cells, and blood vessels have been growing into the pores of the porous HA and the osteoblast is converged onto the skeleton surface of the porous HA to form new bone.

4. Conclusions

(1) With suitable slurry, porous HA bioceramics having interconnecting pores and high porosity (up to 80%) can be obtained by the method of the replication of porous polymeric substrates.

(2) The porosity of HA can be varied easily with different content of the slurry.

(3) The pore size of HA can also be varied freely from selecting different substrates while the largest pore size of substrates was no more than 2 mm.

(4) The compressive strength of porous HA has a exponential tendency with porosity.

(5) The animal experiments show that porous HA possess growing bone ability.

Acknowledgments

We are very grateful to Beijing Fine Ceramic Laboratory, INET, Tsinghua University, for supporting this work.

References

1. K. DE GROOT, *Biomaterials* **1** (1980) 47.
2. M. JARCHO, *Clin. Orthop. Rel. Res.***157** (1981) 259.
3. J. W. FRAME and C. L. BRADY, *Brit. J. Oral Maxillofac. Surg.* **25** (1987) 452.
4. H. GHGUSHI, Y. DOHI, S.TAMAI and S. TABATA, *J. Biomed. Mater. Res.* **27** (1993) 1401.
5. R. E. HOLMES, V. MOONEY, R. BUCHOLZ and A. TENCER, *Clin. Orthop. Rel. Res.* **188** (1984) 252.
6. S. F. HULBERT, R. S. YOUNG and J. J. KLAWITTER. *J. Biomed. Mater. Res.* **4** (1970).
7. J. J. KLAWITTER and S. F. HULBERT, *ibid.* **5** (1971).
8. S. F. HULBERT, S. J. MORRISON and J. J. KLAWITTER, *J. Biomed. Mater. Res. Symp.* **2** (1) (1970) 269.
9. P. SEPULVEDA, *Amer. Ceram. Soc. Bull.* **76** (10) (1997) 62.
10. RAVAULT, US. Patent no. 3 907 579, Sept. 23, 1975.
11. R. W. RICE, in "Treatice in Material Science and Technology," Vol. 11 edited by R. K. MacCrone (Academic Press, New York, 1977) p. 200.

Received 2 April 1999
and accepted 11 April 2000